J. Am. Ceram. Soc., 94 [4] 969–972 (2011)
DOI: 10.1111/j.1551-2916.2010.04257.x

journal

Three-Dimensional Printing of Ti_3SiC_2-Based Ceramics

Beiya Nan, Xiaowei Yin,† Litong Zhang, and Laifei Cheng

National Key Laboratory of Thermostructure Composite Materials, Northwestern Polytechnical University, Xi'an, Shaanxi 710072, China

In the present work, we explored the feasibility of fabricating Ti_3SiC_2-based ceramics by a near-net-shape fabrication process of three-dimensional printing (3D printing) combined with liquid silicon infiltration (LSI). The porous ceramic preform was fabricated by 3D printing TiC powder with dextrin as a binder. The heat-treated preforms contained bimodal pore structure with interagglomerate pores ($d \approx 23$ μm) and intraagglomerate pores ($d \approx 1$ μm). Upon infiltration in Ar atmosphere at 1600°–1700°C for 1 h, silicon melt infiltrated the pores and reacted with TiC to yield Ti_3SiC_2, $TiSi_2$, and SiC. The effects of silicon content and infiltration temperature on the phase composition of the Ti_3SiC_2-based composites were also studied. After LSI at 1700°C for 1 h, the composites with an initial TiC:Si mole ratio of 3:1.2 attained a bending strength of 293 MPa, a Vickers hardness of 7.2 GPa, and an electrical resistivity of 27.8 μΩ·cm, respectively.

I. Introduction

THE $TiSi_2$ possesses low density (4.04 g/cm^3), moderate melting point (1540°C), high elastic modulus (250 GPa),[1] high oxidation resistance (1200°–1300°C), and low electrical resistivity (13–16 μΩ·cm),[2] which receives considerable attention for potential applications as a high-temperature material and electronic interconnections. However, low fracture toughness (2–3 MPa·m$^{1/2}$)[1] and strength (170 MPa) greatly limit its potential applications.[3] As a representative nanolaminated ternary carbide,[4] Ti_3SiC_2 has high melting point, low density (4.53 g/cm^3), low hardness (Vickers hardness of 4 GPa),[5] excellent thermal shock resistance,[6] high strength (bending strength 475 MPa),[7] high fracture toughness (K_{Ic} = 8–16 MPa·m$^{1/2}$) depending on the grain size,[5,8] and low electrical resistivity (22 μΩ·cm).[4] Because Ti_3SiC_2 is relatively soft, hard materials such as TiC and SiC have been combined to improve its hardness.[7,9] Recently, the thermal stability of Ti_3SiC_2–TiC–$TiSi_2$ composite in vacuum has been investigated.[10] It was revealed that Ti_3SiC_2–TiC–$TiSi_2$ composites were thermally stable at temperatures up to 1300°C. The combination of Ti_3SiC_2, SiC, TiC, and $TiSi_2$ may produce a composite with not only high mechanical properties and good oxidation resistance but also low electrical resistivity.

Three-dimensional printing (3D printing) is a promising additive manufacturing technology, which can create complex-shape ceramic parts that cannot be produced by traditional approaches.[11,12] While 3D printing may produce porous preforms with a high degree of freedom in geometry and shape, capillary-driven infiltration of the metal melt followed by a subsequent reaction in the composite material may result in a dense microstructure of the component. Nanolaminated Ti_3AlC_2 toughened $TiAl_3$–Al_2O_3 composites have been fabricated by a combination process of 3D printing and aluminum melt reactive infiltration,[13] which exhibited rising *R*-curve behavior with extensive crack deflection along the (0001) lamellar sheets of Ti_3AlC_2.

In this work, for the first time, Ti_3SiC_2-based composite was fabricated using a combination process of 3D printing and liquid silicon infiltration (LSI). Effects of silicon content and infiltration temperature on the microstructure and mechanical properties of Ti_3SiC_2-based ceramic were studied.

II. Experimental Procedure

(1) Materials Preparation

A 90 wt% TiC powder (average particle size: 1.5 μm, >99% purity, Longjin Co. Ltd., Shanghai, China) and 10 wt% dextrin powder ($(C_6H_{10}O_5)_n \cdot xH_2O$, average particle size: 115 μm, Hedong Hongyan, Tianjin, China) were mixed in distilled water and ball milled for 12 h. The as-received slurry was dried using a freeze drier (LGJ-18S, SongYuan HuaXing Co. Ltd., Beijing, China). After dry ball milling, the powder was passed through a 60 mesh sieve. The green bodies were printed using 3D printer (Spectrum Z510, Z Corporation, Burlington, MA), which were subsequently heat-treated in flowing argon at 1400°C for 1 h in an Al_2O_3 tube furnace (Kejing Co. Ltd., Hefei, China). During the heat treatment process, the dextrin was decomposed into pyrolysis carbon.

LSI was conducted in a high-temperature furnace (HT 1800 M-Plus, Linn High Therm GmbH, Eschenfelden, Bayern, Germany) in an Ar atmosphere. The heat-treated preforms were infiltrated with silicon at 1600°–1700°C for 1 h, and then annealed at 1400°C for 2 h, and the initial TiC:Si mole ratio in the infiltrated preforms was controlled to be 3:0.7, 3:0.9, and 3:1.2, respectively. The heating and cooling rates were 10 and 2°C/min, respectively.

(2) Characterization

The relative density and open porosity of the samples were measured by the Archimedes' method. The pore size distribution was measured using a Mercury Poremaster (Poremaster 33, Quantachrome Instruments Co. Boynton Beach, FL). The electrical resistivity was measured by the four-probe method using a Quantum Design (Versa Lab, San Diego, CA). The microstructure of the fractured surfaces was observed by scanning electron microscopy (SEM, S-2700, Hitachi, Tokyo, Japan), and the elemental analysis was conducted by energy-dispersive spectroscopy (EDS). Hardness was measured using a Vickers hardness machine (HBV-30A, Huayin Co. Ltd., Laizhou, China) using 100 N load with a dwell time of 15 s. The samples with a dimension of 3 mm × 4 mm × 35 mm were used to test the three-point bending strength using an Instron universal testing machine (CMT 4304, Sans Materials Testing Co. Ltd., Shenzhen, China). The span was 30 mm and the cross-head speed was 0.5 mm/min. Infiltrated samples were also crushed into a powder and analyzed by X-ray diffractometry (XRD, Rigaku D/max-2400, Tokyo, Japan) with Cu*K*α radiation at 40 kV and 100 mA.

N. Travitzky—contributing editor

Manuscript No. 28670. Received September 26, 2010; approved October 14, 2010.
This work was financially supported by the Natural Science Foundation of China (Grant: 50802074) and the 111 Project (B08040).
†Author to whom correspondence should be addressed. e-mail: yinxw@nwpu.edu.cn

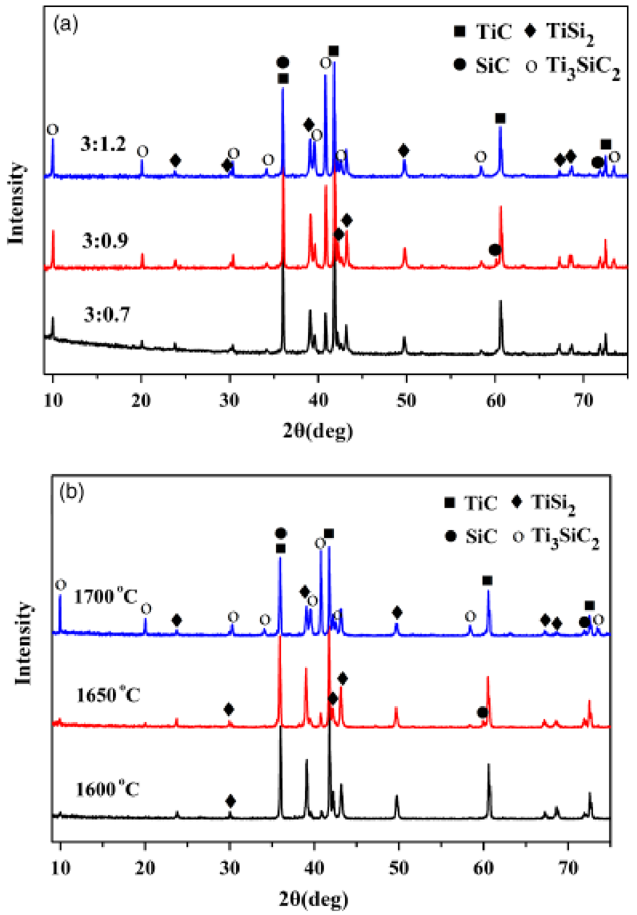

Fig. 1. X-ray diffraction patterns of (a) the composites with various mole ratios of TiC:Si (3:0.7, 3:0.9, 3:1.2) reacting at 1700°C for 1 h, and (b) the composites with the same reaction mole ratio of 3TiC/1.2Si reacting at different infiltration temperatures (1600°, 1650°, and 1700°C) for 1 h.

The content of the individual phases in the synthesized composites can be estimated from the integrated XRD peak intensities using direct comparison method.[14]

III. Results and Discussion

The heat-treated preform had the representative bimodal pore size structure with intraagglomerate pores ($d \approx 1$ μm) and interagglomerate pores ($d \approx 23$ μm), which was the typical microstructure of 3D printing preform.[11] The relative density and open porosity of the heat-treated preform were 1.58 g/cm^3 and 66%, respectively. The bimodal pore structure favors LSI.[15]

Figures 1(a) and (b) show the XRD patterns of the composites after LSI. All of the composites were composed of Ti_3SiC_2, $TiSi_2$, TiC, and SiC. When the mole ratio of TiC:Si shifted from 3:0.7 to 3:1.2, the volume content of Ti_3SiC_2 greatly increased with the increasing Si content (Fig. 2(a)). The composites with initial composition 3TiC/0.7Si, 3TiC/0.9Si, and 3TiC/1.2Si contained 29, 33, and 45 vol% Ti_3SiC_2, respectively. There were large amounts of residual TiC, because the Si content was insufficient to completely react with TiC. With the increase of Si content, the content of SiC did not increase. This implies that the following reaction may be preferred to occur:

$$\mathrm{Ti-Si}(l) + \mathrm{TiC}(s) \rightarrow \mathrm{Ti_3SiC_2}(s)$$

With raising Si content, the content of Ti–Si liquid was improved from the eutectic reaction of Si–$TiSi_2$ at temperatures above 1330°C.[16] Ti–Si liquids spread over TiC particles, resulting in the rearrangement of particles and formation of Ti_3SiC_2,

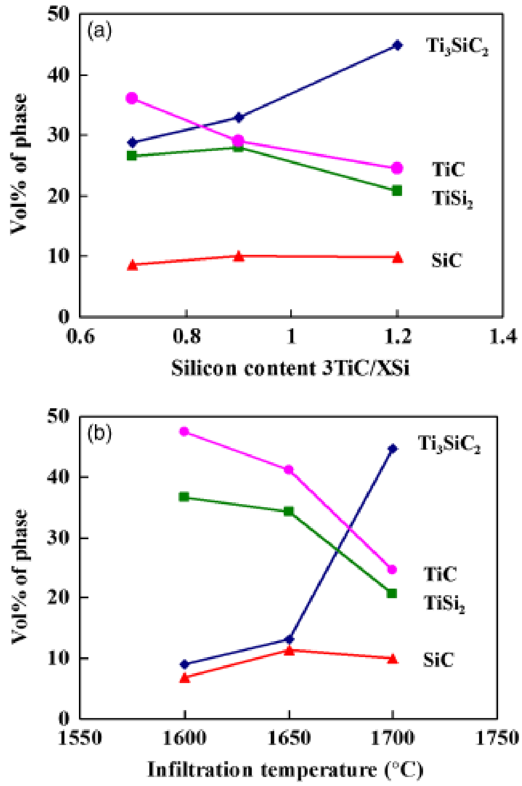

Fig. 2. Phase contents of the final products evaluated with respect to (a) silicon content of the starting powder infiltrated at 1700°C for 1 h, and (b) different infiltration temperatures (1600°, 1650°, and 1700°C) with the same reaction mole ratio of 3TiC/1.2Si for 1 h.

which may be facilitated by raising the infiltration temperature. When TiC:Si mole ratio was 3:1.2, the Ti_3SiC_2 content increased from 9 to 45 vol% with the increase of infiltration temperature from 1600° to 1700°C, while TiC and $TiSi_2$ contents decreased from 48 to 25 vol%, and 37 to 21 vol%, respectively.

The low-magnification BSE images are shown in Figs. 3(a)–(c). When the infiltration temperature increased from 1600° to 1700°C, Ti_3SiC_2 content increased obviously, which was consistent with the XRD analysis. Figure 3(d) shows an enlarged micrograph of the "I" area marked in Fig. 3(a). EDS analysis confirmed that the white phase was Ti_3SiC_2, the continuous gray phase was $TiSi_2$, the black phase was SiC, and the white-gray phase was TiC.

Table I presents the properties of the composites with the mole ratio of 3TiC/1.2Si. The maximum Vickers hardness and electrical resistivity of Ti_3SiC_2-based ceramics containing 48 vol% TiC could reach 10.8 GPa and 56.8 μΩ·cm, respectively, which was attributed to the higher Vickers hardness (28–35 GPa)[17] and electrical resistivity (62.5 μΩ·cm) of TiC,[18] compared with those of Ti_3SiC_2. With the increase of infiltration temperature, the bending strength increased, which was attributed to the increase of Ti_3SiC_2 content and the decrease of open porosity. The typical damage mechanisms of delamination, laminate fracture, buckling, and kink band can be observed in the SEM micrographs of fractured surfaces (Fig. 4). These mechanisms of damage belong to multiple energy-absorbing mechanisms and favor the improvement of strength and fracture toughness of the materials.[19] In this work, the maximum bending strength and the minimum electrical resistivity of the composites could achieve 293 MPa and 27.8 μΩ·cm, respectively, owing to the high content of Ti_3SiC_2.

IV. Conclusion

Ti_3SiC_2-based ceramics could be synthesized by combining 3D printing with LSI process. The amount of Ti_3SiC_2 was highly

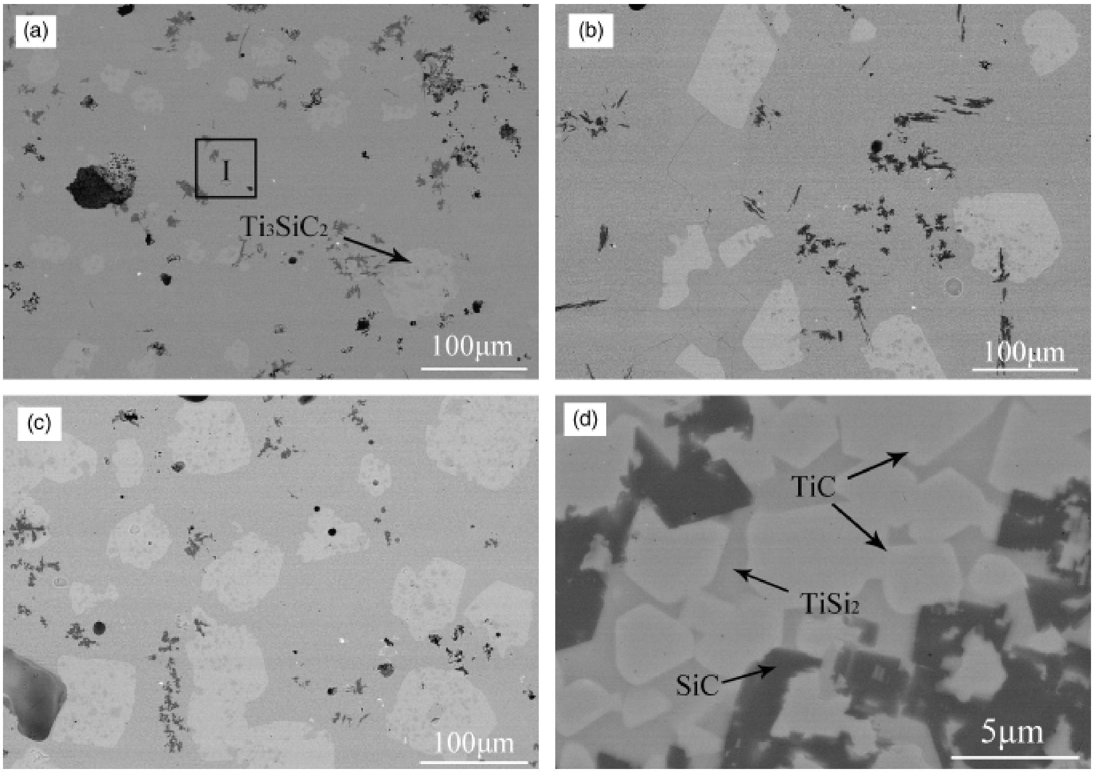

Fig. 3. BSE images taken from the polished surfaces of the composites infiltrated at (a) 1600°C, (b) 1650°C, (c) 1700°C, and (d) higher magnification micrograph taken from "I" area marked in (a).

Table I. Properties of the Composites with the Same Reaction Mole Ratio of 3TiC/1.2Si

Infiltration temperature (°C)	Density (g/cm^3)	Open porosity (%)	Electrical resistivity (μΩ·cm)	Vickers hardness (GPa)	Bending strength (MPa)
1600	4.08	8	56.8±0.3	10.8±1	52±2
1650	4.17	3.6	49.5±0.5	9.6±0.5	166±7.5
1700	4.24	2.4	27.8±1	7.2±0.4	293±17.8

dependent on the infiltration temperature and the content of Si introduced into the preforms. The composite with the highest amount (45 vol%) of Ti_3SiC_2 was fabricated by LSI with an initial TiC:Si mole ratio of 3:1.2 reacting at 1700°C for 1 h, which attained a bending strength of 293 MPa, a Vickers hardness of 7.2 GPa, and an electrical resistivity of 27.8 μΩ·cm, respectively.

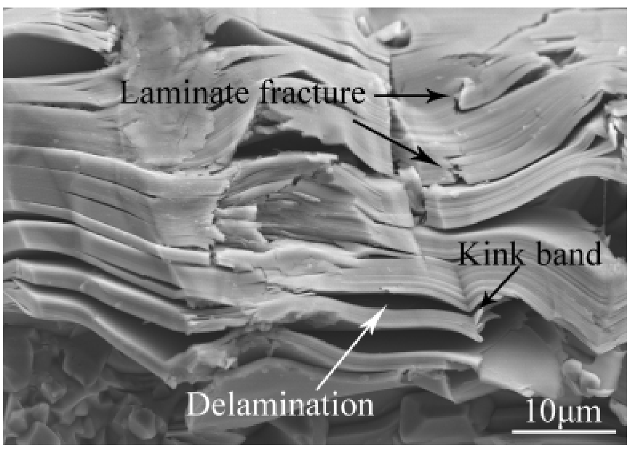

Fig. 4. Scanning electron microscopic image of fractured surface of the composite infiltrated at 1700°C showing typical damage mechanisms.

References

[1]T. S. R. Ch. Murthy, C. Subramanian, R. K. Fotedar, M. R. Gonal, P. Sengupta, S. Kumar, and A. K. Suri, "Preparation and Property Evaluation of TiB_2+$TiSi_2$ Composite," *Int. J. Refract. Met. Hard Mater.*, **27** [3] 629–36 (2009).

[2]S. P. Murarka, "Silicide Thin Films and Their Applications in Microelectronics," *Intermetallics*, **3** [3] 173–86 (1995).

[3]J. L. Li, D. L. Jiang, and S. H. Tan, "Microstructure and Mechanical Properties of In Situ Produced SiC/$TiSi_2$ Nanocomposites," *J. Eur. Ceram. Soc.*, **20** [2] 227–33 (2000).

[4]M. W. Barsoum, "The $M_{N+1}AX_N$ Phases: A New Class of Solids; Thermodynamically Stable Nanolaminates," *Prog. Solid State Chem.*, **28** [1–4] 201–81 (2000).

[5]C. J. Gilbert, D. R. Bloyer, M. W. Barsoum, T. El-Raghy, A. P. Tomsia, and R. O. Ritchie, "Fatigue-Crack Growth and Fracture Properties of Coarse and Fine-Grained Ti_3SiC_2," *Scr. Mater.*, **42**, 761–7 (2000).

[6]H. B. Zhang, Y. C. Zhou, Y. W. Bao, and M. S. Li, "Abnormal Thermal Shock Behavior of Ti_3SiC_2 and Ti_3AlC_2," *J. Mater. Res.*, **21** [9] 2401–7 (2006).

[7]D. T. Wan, Y. C. Zhou, Y. W. Bao, and C. K. Yan, "In Situ Reaction Synthesis and Characterization of $Ti_3Si(Al)C_2$/SiC Composites," *Ceram. Int.*, **32** [8] 883–90 (2006).

[8]D. Chen, K. Shirato, M. W. Barsoum, T. El-Raghy, and R. O. Ritchie, "Cyclic Fatigue-Crack Growth and Fracture Properties in Ti_3SiC_2 Ceramics at Elevated Temperatures," *J. Am. Ceram. Soc.*, **84** [12] 2914–20 (2001).

[9]S. Konoplyuk, T. Abe, T. Uchimoto, and T. Takagi, "Synthesis of Ti_3SiC_2/TiC Composites from TiH_2/SiC/TiC Powders," *Mater. Lett.*, **59** [18] 2342–6 (2005).

[10]W. K. Pang, I. M. Low, B. H. O'Connor, A. J. Studer, V. K. Peterson, and J. P. Palmquist, "Effect of Vacuum Annealing on the Thermal Stability of Ti_3SiC_2/TiC/$TiSi_2$ Composites," *J. Aust. Ceram. Soc.*, **45** [1] 72–7 (2009).

[11]X. W. Yin, N. Travitzky, and P. Greil, "Near-Net-Shape Fabrication of Ti_3AlC_2-Based Composites," *Int. J. Appl. Ceram. Technol.*, **4** [2] 184–90 (2007).

[12]M. C. Melican, M. C. Zimmerman, M. S. Dhillon, A. R. Ponnambalam, A. Curodeau, and J. R. Parsons, "Three-Dimensional Printing and Porous Metallic Surfaces: A New Orthopedic Application," *J. Biomed. Mater. Res.*, **55** [2] 194–202 (2001).

[13]X. W. Yin, N. Travitzky, and P. Greil, "Three-Dimensional Printing of Nanolaminated Ti_3AlC_2 Toughened $TiAl_3$–Al_2O_3 Composites," *J. Am. Ceram. Soc.*, **90** [7] 2128–34 (2007).

[14]I. Kero, R. Tegman, and M. L. Antti, "Effect of the Amounts of Silicon on the In Situ Synthesis of Ti_3SiC_2 Based Composites Made from TiC/Si Powder Mixtures," *Ceram. Int.*, **36** [1] 375–9 (2010).

[15]X. W. Yin, N. Travitzky, R. Melcher, and P. Greil, "Three-Dimensional Printing of $TiAl_3$/Al_2O_3 Composites," *Int. J. Mater. Res.*, **97** [5] 492–8 (2006).

[16]X. Yin, K. X. Chen, H. P. Zhou, and X. S. Ning, "Combustion Synthesis of Ti_3SiC_2/TiC Composites from Elemental Powders Under High-Gravity Conditions," *J. Am. Ceram. Soc.*, **93** [8] 2182–7 (2010).
[17]W. B. Tian, Z. M. Sun, H. Hashimoto, and Y. L. Du, "Microstructural Evolution and Mechanical Properties of Ti_3SiC_2–TiC Composites," *J. Alloys Compd.*, **502** [1] 49–53 (2010).
[18]M. W. Barsoum and T. El-Raghy, "Synthesis and Characterization of a Remarkable Ceramic: Ti_3SiC_2," *J. Am. Ceram. Soc.*, **79** [7] 1953–6 (1996).
[19]I. M. Low, S. K. Lee, and B. R. Lawn, "Contact Damage Accumulation in Ti_3SiC_2," *J. Am. Ceram. Soc.*, **81** [1] 225–8 (1998). □